JCI The Journal of Clinical Investigation

Amendment history:
- Corrigendum (October 2006)

Alzheimer disease β-amyloid activity mimics cholesterol oxidase

Luigi Puglielli, … , Dora M. Kovacs, Ashley I. Bush

J Clin Invest. 2005;115(9):2556-2563. https://doi.org/10.1172/JCI23610.

Research Article **Neuroscience**

The abnormal accumulation of amyloid β-peptide (Aβ) in the form of senile (or amyloid) plaques is one of the main characteristics of Alzheimer disease (AD). Both cholesterol and Cu^{2+} have been implicated in AD pathogenesis and plaque formation. Aβ binds Cu^{2+} with very high affinity, forming a redox-active complex that catalyzes H_2O_2 production from O_2 and cholesterol. Here we show that Aβ:Cu^{2+} complexes oxidize cholesterol selectively at the C-3 hydroxyl group, catalytically producing 4-cholesten-3-one and therefore mimicking the activity of cholesterol oxidase, which is implicated in cardiovascular disease. Aβ toxicity in neuronal cultures correlated with this activity, which was inhibited by Cu^{2+} chelators including clioquinol. Cell death induced by staurosporine or H_2O_2 did not elevate 4-cholesten-3-one levels. Brain tissue from AD subjects had 98% more 4-cholesten-3-one than tissue from age-matched control subjects. We observed a similar increase in the brains of Tg2576 transgenic mice compared with nontransgenic littermates; the increase was inhibited by in vivo treatment with clioquinol, which suggests that brain Aβ accumulation elevates 4-cholesten-3-one levels in AD. Cu^{2+}-mediated oxidation of cholesterol may be a pathogenic mechanism common to atherosclerosis and AD.

Alzheimer disease β-amyloid activity mimics cholesterol oxidase

Luigi Puglielli,[1] Avi L. Friedlich,[2] Kenneth D.R. Setchell,[3] Seiichi Nagano,[2] Carlos Opazo,[4] Robert A. Cherny,[4] Kevin J. Barnham,[4] John D. Wade,[5] Simon Melov,[6] Dora M. Kovacs,[1] and Ashley I. Bush[2,4]

[1]Neurobiology of Disease Laboratory and [2]Laboratory for Oxidation Biology, Genetics and Aging Research Unit, Massachusetts General Hospital, Harvard Medical School, Charlestown, Massachusetts, USA. [3]Department of Pathology, Cincinnati Children's Hospital Medical Center, University of Cincinnati College of Medicine, Cincinnati, Ohio, USA. [4]Mental Health Research Institute of Victoria and Department of Pathology and [5]Howard Florey Institute of Medical Research, University of Melbourne, Parkville, Victoria, Australia. [6]Buck Institute for Age Research, Novato, California, USA.

The abnormal accumulation of amyloid β-peptide (Aβ) in the form of senile (or amyloid) plaques is one of the main characteristics of Alzheimer disease (AD). Both cholesterol and Cu^{2+} have been implicated in AD pathogenesis and plaque formation. Aβ binds Cu^{2+} with very high affinity, forming a redox-active complex that catalyzes H_2O_2 production from O_2 and cholesterol. Here we show that Aβ:Cu^{2+} complexes oxidize cholesterol selectively at the C-3 hydroxyl group, catalytically producing 4-cholesten-3-one and therefore mimicking the activity of cholesterol oxidase, which is implicated in cardiovascular disease. Aβ toxicity in neuronal cultures correlated with this activity, which was inhibited by Cu^{2+} chelators including clioquinol. Cell death induced by staurosporine or H_2O_2 did not elevate 4-cholesten-3-one levels. Brain tissue from AD subjects had 98% more 4-cholesten-3-one than tissue from age-matched control subjects. We observed a similar increase in the brains of Tg2576 transgenic mice compared with nontransgenic littermates; the increase was inhibited by in vivo treatment with clioquinol, which suggests that brain Aβ accumulation elevates 4-cholesten-3-one levels in AD. Cu^{2+}-mediated oxidation of cholesterol may be a pathogenic mechanism common to atherosclerosis and AD.

Introduction

Oxidation of cholesterol, which is catalyzed by redox-active metals such as Cu^{2+}, may play an important role in atherogenesis (1–4). The risk for Alzheimer disease (AD) is related to hypercholesterolemia by mechanisms involving oxidative stress that are still unclear (5, 6). AD is characterized by amyloid β-peptide (Aβ) accumulation in the neocortex, which is linked to peroxidative damage (7, 8) and is also observed in Aβ-expressing transgenic mice (9). Aβ is a 39- to 43-aa peptide that binds Cu^{2+} with high affinity (10–13). The Aβ:Cu^{2+} complex is redox active, producing neurotoxic H_2O_2 from O_2 through the reduction of Cu^{2+}, and may cause the oxidative damage observed in AD brain tissue (14, 15). The Aβ:Cu^{2+} complex (1:2 ratio) binds cholesterol within lipid membranes (13) and can recruit cholesterol as a reducing agent for the catalytic production of H_2O_2 in vitro (15). While these in vitro data suggest a plausible atherogenesis-like mechanism linking cholesterol to Aβ in AD, so far there has been no evidence to our knowledge for such biochemistry occurring in the disease.

Oxidation of cholesterol, which resembles atherogenesis, has been proposed as a pathogenic event in AD (2, 6). For example, cholesterol ozone derivatives, previously found in atherosclerotic plaques, have been identified in the brain and shown to covalently modify Aβ and accelerate its amyloidogenesis in vitro (16). The brain possesses the highest content of sterols in the body, containing approximately 20% of total body cholesterol while accounting for only approximately 2% of body mass (17). Cholesterol derivatives are enriched in cerebral Aβ deposits in AD and β-amyloid protein precursor (APP) transgenic mice (18), and dietary cholesterol increases cerebral Aβ deposition in APP transgenic mouse models of AD (19, 20). Aβ:Cu^{2+} complexes are also enriched in amyloid plaques in AD (21, 22), and Aβ from AD brain tissue co-purifies with Cu^{2+} and Zn^{2+} but no other metals (15). Therefore, the catalytic machinery to oxidize cholesterol colocalizes with its substrate in the brain in AD.

Here we report that the Aβ:Cu^{2+} complex acts as a novel mammalian cholesterol oxidase, utilizing the hydroxyl group at position 3 of cholesterol to catalytically generate H_2O_2 (Figure 1A). Actual cholesterol oxidase is a bacterial flavoenzyme that is implicated in the ability of bacteria to induce cellular lysis upon infection of their hosts and to induce thrombus (23). Sequence similarity studies have failed to identify a mammalian counterpart, and cholesterol oxidase is generally regarded as unique to bacteria (24). We also found that levels of 4-cholesten-3-one, the product of cholesterol oxidase activity, were significantly elevated in the postmortem brain tissue of subjects with AD compared with age-matched controls; the same result was observed in the brains of Aβ transgenic mice. These findings support the possibility of direct oxidation of cholesterol by Aβ in vivo, which may explain the occurrence of aortic atherosclerosis in Aβ transgenic mice (20). Therefore, AD and atherogenesis may share Cu^{2+}-mediated oxidation of cholesterol as a pathogenic mechanism.

Nonstandard abbreviations used: Aβ, amyloid β-peptide; $Aβ_{42}$His1Met, Aβ with all 3 histidine residues methylated at the π position; $Aβ_{42}$His3Met, Aβ with all 3 histidine residues methylated at the τ position; $Aβ_{42}$Y10A, Aβ with the tyrosine residue at position 10 substituted to alanine; AC, normal age-matched control; AD, Alzheimer disease; amu, atomic mass unit(s); APP, β-amyloid protein precursor; CQ, clioquinol; GC-MS, gas chromatography–mass spectrometry; LDH, lactate dehydrogenase; MU, methylene unit(s); PARP, poly(ADP-ribose) polymerase; PD, age-matched Parkinson disease control; *Rf*, relative migration factor; TETA, triethylenetetramine; TLC, thin layer chromatography; YC, young normal adult control.

Conflict of interest: R.A. Cherny, K.J. Barnham, and A.I. Bush are shareholders in and paid consultants for Prana Biotechnology Ltd., which has an interest in clioquinol, a drug that is mentioned in the text.

Citation for this article: *J. Clin. Invest.* **115**:2556–2563 (2005). doi:10.1172/JCI23610.

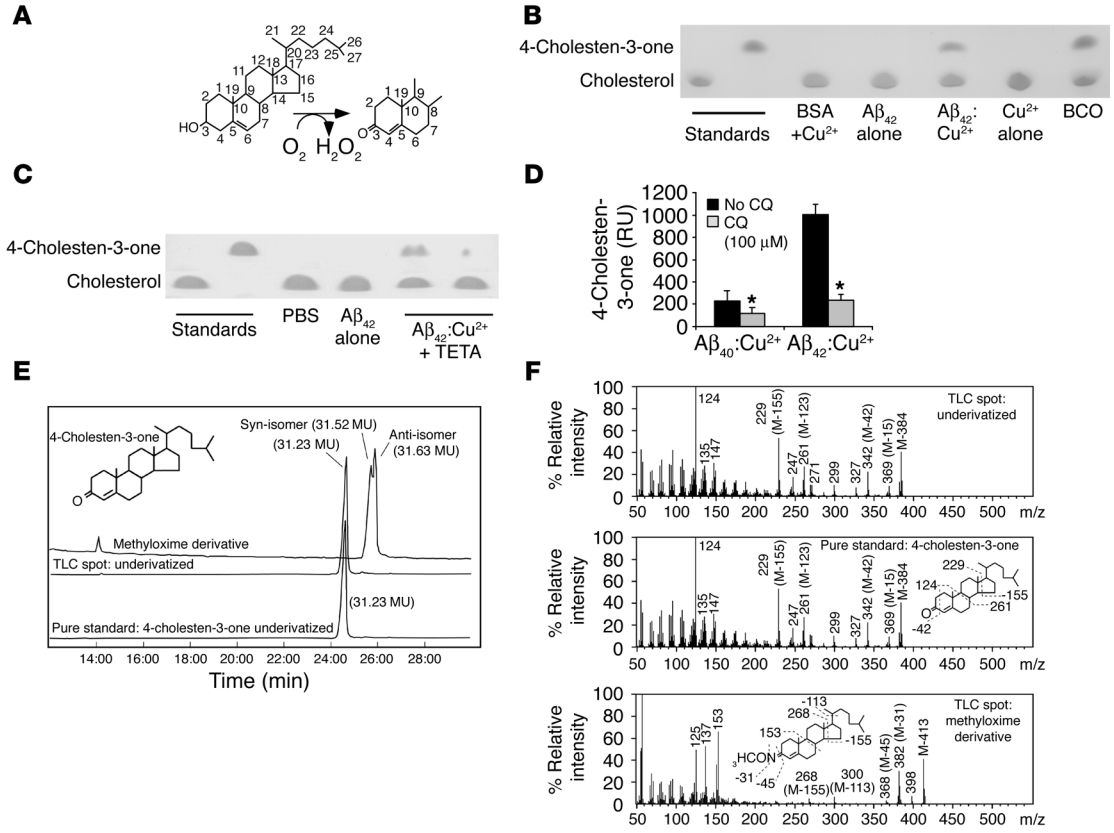

Figure 1

Cholesterol oxidase activity of Aβ:Cu^{2+}. (**A**) Chemical structure of cholesterol showing oxidation of the hydroxyl group at position C-3 by cholesterol oxidase activity. (**B** and **C**) The migrations of nonoxidized cholesterol and 4-cholesten-3-one standards are shown. (**B**) Oxidation of cholesterol (50 μM) after incubation with BSA/Cu^{2+} (1 μM:2 μM), $Aβ_{42}$ (1 μM), Cu^{2+} (2 μM), $Aβ_{42}$:Cu^{2+} complex (1 μM:2 μM), or bacterial cholesterol oxidase (BCO; 5 IU). (**C**) Effect of Cu^{2+} chelation (with 1 mM TETA) on 4-cholesten-3-one generation by the $Aβ_{42}$:Cu^{2+} complex; conditions as in **B**. Data are representative of at least 3 experiments. (**D**) Generation of 4-cholesten-3-one on TLC of $Aβ_{40}$ and $Aβ_{42}$ complexed with Cu^{2+} (1 μM:2 μM), and inhibition by the Cu^{2+} chelator CQ (100 μM). Bars show mean ± SD. Significance was calculated by 2-tailed Student's *t* test of CQ effect. **P* < 0.05. RU, relative units. (**E**) Total ion current mass chromatograms obtained by repetitive scanning GC-MS analysis of the underivatized compound and methyloxime derivative of the sample eluted from the TLC spot were superimposed for comparison with pure standard of 4-cholesten-3-one. The retention indices of each compound are denoted in MU. (**F**) Electron ionization (70 electron volts) mass spectrum of a compound identified as 4-cholesten-3-one by TLC from extracts of AD brain tissue eluted from the TLC plate: underivatized compound (top), 4-cholesten-3-one standard (middle), methyloxime derivative of the TLC extract (bottom; syn-isomer only shown) confirming the expected shift in masses of the molecular and fragment ions.

Results

Aβ:Cu^{2+} acts as a novel cholesterol oxidase in vitro. To characterize the oxidized species of cholesterol formed by Aβ:Cu^{2+}, we incubated free cholesterol in the presence of Aβ, Cu^{2+}, or Aβ:Cu^{2+} complex in vitro. Thin layer chromatography (TLC) revealed 2 distinct spots, one corresponding to free cholesterol substrate (relative migration factor [R*f*] = 0.17) and the other comigrating with 4-cholesten-3-one (R*f* = 0.25), a finding which implies that oxidation of the hydroxyl group occurs at carbon position C-3, a potential electron donor contributing to the reduction of O_2 during H_2O_2 generation (Figure 1, A and B). These R*f* values were in agreement with previously published values (25) and confirmed using pure standards of cholesterol and 4-cholesten-3-one (Figure 1B). Bacterial cholesterol oxidase, which generates 4-cholesten-3-one from cholesterol, produced a single spot that migrated with identical R*f* to that of Aβ:Cu^{2+} (Figure 1B). We did not detect additional spots by TLC. We therefore confirmed that H_2O_2 was generated by Aβ:Cu^{2+} during the oxidation of cholesterol, as previously reported (15).

Neither Aβ, nor free Cu^{2+}, nor Cu^{2+} bound to BSA (a redox-suppressing, Cu^{2+}-binding protein) (26) oxidized cholesterol under these conditions (Figure 1B). The Cu^{2+} chelator triethylenetetramine (TETA) inhibited 4-cholesten-3-one generation by Aβ:Cu^{2+}, which confirms the requirement for Cu^{2+} in mediating the reaction (Figure 1C).

The longer hydrophobic carboxyl terminus enhances the stability of the hexameric $Aβ_{42}$:Cu^{2+} structure compared with that of $Aβ_{40}$:Cu^{2+} (12) and increases the peptide's Cu^{2+} affinity, redox activity, H_2O_2 production, and toxicity (10, 11, 15). Consistent with these results, we found that $Aβ_{42}$ is approximately 5 times more active than $Aβ_{40}$ in generating 4-cholesten-3-one (Figure 1D). Nevertheless, the $Aβ_{40}$:Cu^{2+} complex did generate significant amounts of 4-cholesten-3-one. As with TETA (Figure 1C), the Cu^{2+} chelator clioquinol (CQ), which is being investigated in clinical trials (27, 28), significantly inhibited the oxidation of cholesterol by both $Aβ_{40}$:Cu^{2+} and $Aβ_{42}$:Cu^{2+} (Figure 1D).

The identity of the 4-cholesten-3-one product was confirmed by gas chromatography–mass spectrometry (GC-MS; Figure 1, E and F).

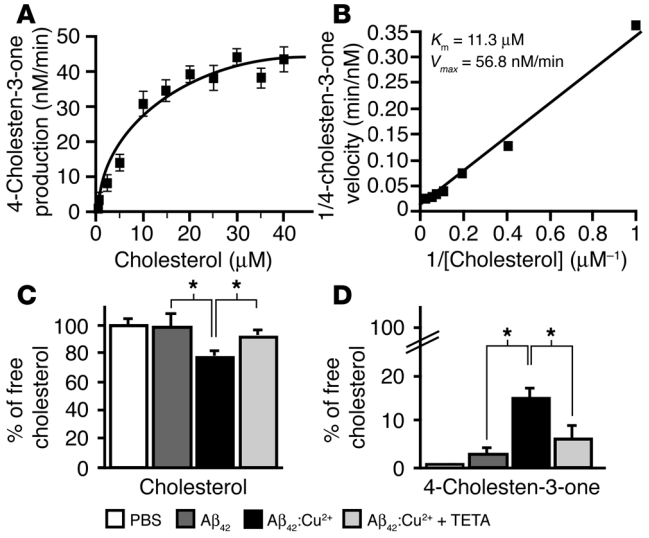

Figure 2
Catalytic oxidation of cell-free and cellular cholesterol by Aβ:Cu^{2+}. (**A**) Production of 4-cholesten-3-one by $A\beta_{42}$:Cu^{2+} (200 nM:400 nM) upon incubation for 60 minutes with increasing concentrations of nonoxidized cholesterol. Experiments were performed in triplicate. (**B**) Lineweaver-Burk transformation of the data shown in **A**. (**C**) Free cholesterol and (**D**) 4-cholesten-3-one in primary neurons after incubation for 2 days with $A\beta_{42}$ (200 nM) and $A\beta_{42}$:Cu^{2+} (200 nM:400 nM) with or without TETA (50 μM). Data are mean ± SD of 4 experiments. *$P < 0.05$.

Figure 1E shows superimposed GC-MS profiles of the TLC-isolated compound in both its underivatized and methyloxime derivative forms from the analysis of AD-affected postmortem brain. In the underivatized sample, a single peak was observed in the GC-MS profile, with a retention index (31.23 methylene units [MU]) identical to the pure 4-cholesten-3-one standard (31.23 MU). When coinjected with the pure standard, a single homogeneous peak resulted (data not shown). The electron ionization mass spectra of the underivatized TLC-extracted spot and pure 4-cholesten-3-one exhibited identical fragmentation patterns (Figure 1F). The molecular ion of the human compound was at m/z 384, which is consistent with the molecular ion of 4-cholesten-3-one. The base peak in both spectra, m/z 124, is characteristic of steroids with a Δ^4-3-one structure and arises from the rupture of the carbon bonds 9-10 and 6-7 with the transfer of 2 hydrogen atoms from C-8 and C-11 (29, 30). This ion is accompanied by the corresponding fragment at m/z 261 (M-123). Further evidence in support of a Δ^4-3-one construction is provided by the ion at m/z 342 that arises from the loss of 42 atomic mass units (amu) caused by elimination of ketene from the A-ring. The ion at m/z 229, representing a loss of 155 amu, is caused by a D-ring cleavage with loss of the cholesterol side chain and carbons C-15, C-16, and C-17 and establishes a C_8 side chain typical of a C_{27} sterol. Identical minor fragmentations and loss of angular methyl groups (loss of 15 amu) were evident in both spectra. The mass spectrum of the underivatized TLC spot was also consistent with a previously published mass spectrum of underivatized 4-cholesten-3-one (31).

Further confirmation of the identity of the TLC spot was established by comparing the mass spectrum and retention indices of the methyloxime derivatives (32) of the sample and standard. Due to the asymmetric nitrogen atom in this derivative, distinct geometric isomers of the syn- and anti- type are formed of steroids having a Δ^4-3-one group that are partially resolved by capillary GC-MS (Figure 1E) (33). The retention indices of the 2 isomers were 31.52 MU (syn-isomer) and 31.63 MU (anti-isomer) for the methyloxime derivatives of 4-cholesten-3-one standard (data not shown) and for the methyloxime derivatives of the AD brain sample material (Figure 1E). The characteristic 31-amu loss ([–OCH_3]) from the molecular ion seen in methyloxime derivatives of steroids accounts for the fragment at m/z 382 in the mass spectrum (Figure 1F). The A-ring fragment and base peak at m/z 124 in the underivatized compound is expectedly shifted to m/z 153 in the derivative due to the presence of the methyloxime. The triplet of ions at m/z 125, m/z 137, and m/z 153 are typical of methyloxime derivatives of steroids possessing the Δ^4-3-one structure in the AB-rings (34). These GC-MS analyses establish conclusively that the identity of the compound eluted from the spot visualized by TLC is 4-cholesten-3-one.

To characterize the catalytic conversion of [^{3}H]cholesterol into 4-cholesten-3-one, we incubated Aβ:Cu^{2+} (200 nM Aβ; 400 nM Cu^{2+}) with increasing concentrations of cholesterol (holding the concentration of [^{3}H]cholesterol constant). The oxidation of cholesterol during the 60-minute incubation period was saturable and dependent on cholesterol concentration, conforming to Michaelis-Menten relationships (Figure 2A). Lineweaver-Burk analysis (Figure 2B) revealed a linear relationship ($r^2 = 0.99$) between $1/V$

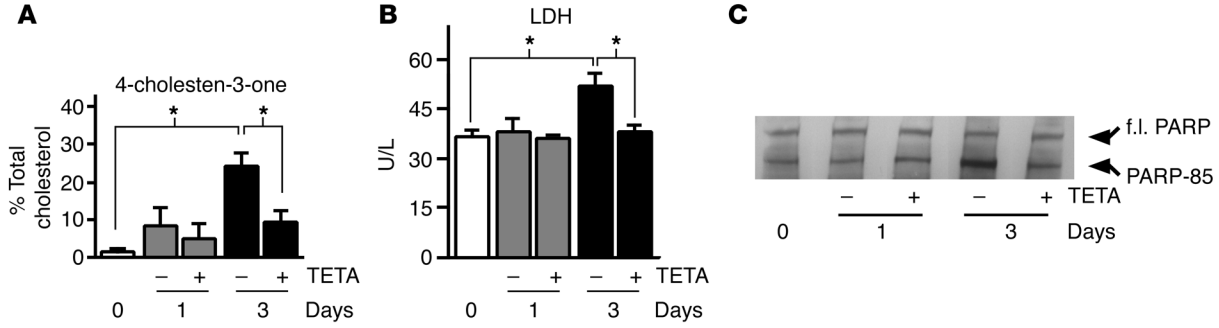

Figure 3
Aβ:Cu^{2+}-induced cholesterol oxidation correlates with toxicity in neuronal cultures. Hippocampal primary neurons were incubated with $A\beta_{42}$:Cu^{2+} (200 nM:400 nM) with or without TETA (50 μM) for the indicated times. (**A**) Effect on 4-cholesten-3-one generation. (**B**) Effect on LDH release in the conditioned media. *$P < 0.05$. (**C**) Effect on the cleavage of full-length PARP (f.l. PARP; 116 kDa) into 85-kDa apoptosis-related (PARP-85) isoforms of PARP. Data are mean ± SD of 3 experiments.

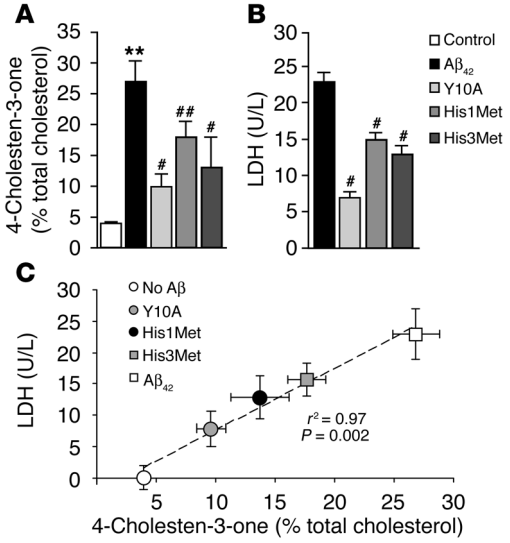

Figure 4
Modified forms of Aβ with diminished toxicity form less 4-cholesten-3-one in neuronal cultures. Hippocampal primary neurons were incubated with $A\beta_{42}$ variants (200 nM) plus Cu^{2+} (400 nM) for 3 days. (**A**) Effect on 4-cholesten-3-one generation. (**B**) Effect on LDH release in the conditioned media. $^{**}P < 0.001$ vs. control; $^{\#}P < 0.001$ vs. $A\beta_{42}$; $^{\#\#}P < 0.01$ vs. $A\beta_{1-42}$. (**C**) Association of 4-cholesten-3-one generated in the culture with LDH release. Baseline values of LDL (37.7 U/l) were subtracted for the purposes of illustration. Data are mean ± SEM of 3 experiments.

and $1/M$, a V_{max} of 56.8 nM/min, and a K_m of 11.3 μM. Therefore, we concluded that Aβ:Cu^{2+} acts as a cholesterol oxidase.

Aβ:Cu^{2+} oxidizes cholesterol in cell culture. To determine whether Aβ:Cu^{2+} will oxidize cholesterol in living cells, hippocampal neurons from mice were treated with $A\beta_{42}$:Cu^{2+} for 2 days. $A\beta_{42}$:Cu^{2+}, but not PBS or $A\beta_{42}$ alone, induced oxidation of cellular cholesterol (Figure 2C). The formation of 4-cholesten-3-one was accompanied by a complementary decrease in cellular free (i.e., nonoxidized) cholesterol (Figure 2, C and D). In agreement with the in vitro experiments (Figure 1C), the chelator TETA — which, unlike CQ, does not penetrate cells — inhibited the generation of 4-cholesten-3-one (Figure 2D), sparing cellular cholesterol (Figure 2C). To determine whether 4-cholesten-3-one generation by Aβ:Cu^{2+} in neuronal culture was merely caused by apoptosis or oxidative stress, we treated cells with staurosporine (2 μM) or H_2O_2 (500 μM) for 3 days as controls but observed no increase in 4-cholesten-3-one levels over background.

Bacterial cholesterol oxidase induces cell necrosis and apoptosis by oxidizing cholesterol in the plasma membrane (35, 36). The toxicity of $A\beta_{42}$ in neuronal culture is dependent upon recruitment of Cu^{2+} by the peptide ($A\beta_{42}$ binds Cu^{2+} with greater affinity than $A\beta_{40}$) and abolished by Cu^{2+} chelation (14, 15, 37). Accordingly, when primary hippocampal neurons were exposed to $A\beta_{42}$:Cu^{2+} (200 nM $A\beta_{42}$; 400 nM Cu^{2+}) over 3 days, we observed a correlation among the formation of 4-cholesten-3-one (Figure 3A); the release of lactate dehydrogenase (LDH) into the culture media, which indicates cytosolic leakage (Figure 3B); and the appearance of the 85-kDa form of poly(ADP-ribose) polymerase (PARP), an early marker of apoptosis, which is produced by CPP32/Mch2α-mediated cleavage of 116-kDa PARP (Figure 3C). Inhibition of the cholesterol oxidase activity of $A\beta_{42}$:Cu^{2+} by TETA decreased cellular 4-cholesten-3-one formation and toxicity (Figure 3, A–C). As a positive control we exposed neuronal cells to cholesterol oxidase purified from *Pseudomonas fluorescens* (0.5 IU, 25°C for 10 minutes), which produced a 2-fold increase in LDH release and induced oxidation of approximately 40% of neuronal cholesterol to 4-cholesten-3-one (data not shown).

Decreased cellular toxicity of modified Aβ:Cu^{2+} complexes that do not embed within lipids corresponds with diminished 4-cholesten-3-one generation. Aβ with the tyrosine residue at position 10 substituted to alanine ($A\beta_{42}$Y10A) has diminished toxicity (38). Similarly, Aβ with all 3 histidine residues methylated at either the π ($A\beta_{42}$His1Met) or τ ($A\beta_{42}$His3Met) positions has diminished toxicity (39). Each of these peptides was shown to coordinate Cu^{2+} in a redox-competent manner and to generate H_2O_2 from the Cu^{2+} catalytic center using O_2 and ascorbate as substrates (38, 39). The only prominent distinguishing feature of these modified peptides that could account for their diminished toxicity was that they did not attach to the surface of cells in culture as strongly as wild-type Aβ (38, 39). Since H_2O_2 production from ascorbate could not account for the diminished neurotoxicity of these Aβ-modified peptides (38, 39), we hypothesized that their lack of adherence to cells in culture prevents them from converting cholesterol into neurotoxic 4-cholesten-3-one.

To test this hypothesis, we studied the toxicity and 4-cholesten-3-one production induced by $A\beta_{42}$ compared with $A\beta_{42}$Y10A, $A\beta_{42}$His1Met, and $A\beta_{42}$His3Met peptides in primary hippocampal cell culture. After 3 days in culture, the modified peptides were indeed significantly less toxic than wild-type $A\beta_{42}$ and correspondingly induced less 4-cholesten-3-one in the culture (Figure 4, A and B). Furthermore, there was a significant concordance between 4-cholesten-3-one levels induced by the different $A\beta_{42}$ variants tested and their corresponding levels of LDH ($P = 0.002$; Figure 4C).

4-Cholesten-3-one generation is increased in the brains of AD patients and APP transgenic mice. To determine whether Aβ:Cu^{2+} complexes possess redox activity in AD, we extracted postmortem brain tissue from subjects with AD as well as from non-AD controls (normal age-matched [AC], age-matched Parkinson disease [PD], and young normal adult control [YC] subjects) and measured cholesterol and 4-cholesten-3-one from the same brain region. 4-Cholesten-3-one was detected in AC brain samples at approximately 0.3 mg/g wet wt, which was only about 1.5% of the amount of cholesterol found in the same tissue and was not significantly greater than the level detected in YC tissue. There was a significant 98% elevation in 4-cholesten-3-one in AD brain tissue compared to AC tissue ($P = 0.0003$); the increase was also significant compared with YC (increase of 181%; $P = 0.0002$) and PD (increase of 169%; $P = 0.01$; Figure 5A). There were no differences in levels of unoxidized cholesterol between these clinical groups (Figure 5B). Assay of the brains of Tg2576 transgenic mice revealed a similarly marked increase in 4-cholesten-3-one compared to age-matched nontransgenic littermate controls (increase of 88%; $P = 0.00001$) (Figure 5C), but no difference in cholesterol levels (Figure 5D). The elevation of 4-cholesten-3-one observed in brain tissue of both AD subjects and APP transgenic mice (Figure 5, A and C) strongly suggests that Aβ selectively forms 4-cholesten-3-one in vivo, while normal 4-cholesten-3-one levels in PD indicate that its elevation is not an epiphenomenon of oxidative stress.

Hydrophobic metal chelators that pass the blood-brain barrier, such as CQ (27) and DP-109 (40), markedly decrease brain Aβ burden in APP transgenic mice. To test whether this decrease correlated with a decrease in 4-cholesten-3-one in brain tissue, we assayed Aβ and 4-cholesten-3-one levels in the brains of CQ- or sham-treated APP transgenic mice. There was a significant 55% decrease

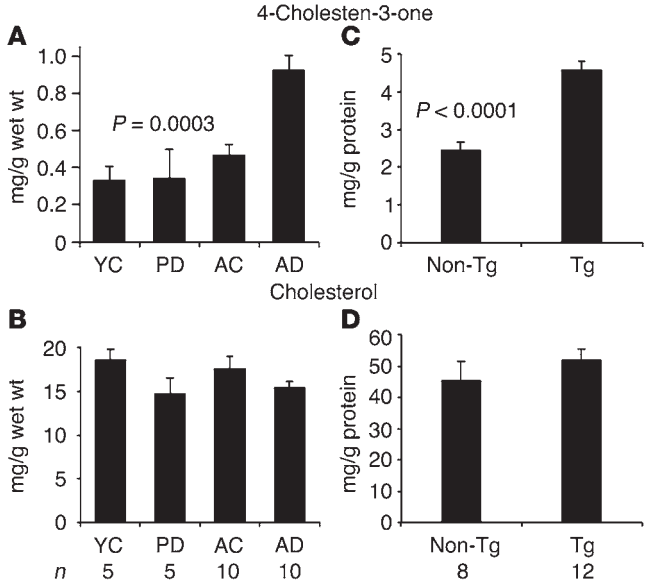

Figure 5

4-Cholesten-3-one is found in the brains of AD patients and AD transgenic mice. 4-cholesten-3-one (**A** and **C**) and nonoxidized cholesterol (**B** and **D**) levels in postmortem brain samples. (**A** and **B**) The inferior parietal lobe, matched for postmortem interval, of YC (age 32.0 ± 11.3 years, 4 males), PD (age 78.2 ± 8.5 years, 3 males), AC (age 78.5 ± 6.9 years, 2 males), and AD subjects (age 78.5 ± 7.5 years, 4 males). *P* value shown is for AD vs. AC subjects. (**C** and **D**) Tg2576 mice and non-Tg littermates (17 months old, 4 females per group).

in the levels of Aβ in the pellet phase of the cerebral hemisphere homogenate of CQ-treated mice (328 ± 28 μg/g wet wt, $n = 6$) compared with controls (733 ± 104 μg/g wet wt, $n = 6$, $P = 0.01$; data not shown), which was accompanied by a significant 46% decrease in 4-cholesten-3-one in the same samples (Figure 6A). Furthermore, there was significant association between the levels of Aβ and the levels of 4-cholesten-3-one in the same samples ($P = 0.02$; Figure 6B), which is compatible with a causal biochemical relationship.

Brain copper levels in the CQ-treated mice did not decrease, but rather increased 14% (CQ, 3.48 ± 0.14 μg/g wet wt, $n = 6$; sham-treated, 3.05 ± 0.12 μg/g wet wt, $n = 6$; $P = 0.04$). Therefore, it is unlikely that the decrease in brain 4-cholesten-3-one in the CQ-treated mice is due to a decrease in brain copper levels indirectly inhibiting oxidation.

Discussion

Our results indicate that the Aβ:Cu^{2+} complex acts as a novel mammalian cholesterol oxidase in vitro and in vivo by using the hydroxyl group at position 3 of cholesterol to catalytically generate H_2O_2 (Figure 1). The cholesterol oxidase activity of Aβ:Cu^{2+} requires Cu^{2+} and is saturable ($K_m = 11.3$ μM, $V_{max} = 56.8$ nM/min; Figure 2, A and B). $Aβ_{42}$:Cu^{2+} induced the generation of 4-cholesten-3-one in primary neurons (Figure 2, C and D, and Figure 3), which correlates with the activation of the apoptotic cascade and the induction of cell toxicity (Figure 3). Cu^{2+} chelation inhibited both 4-cholesten-3-one generation and neuronal death (Figure 2, C and D, and Figure 3).

Our findings implicate the catalytic oxidation of cholesterol to form 4-cholesten-3-one as a component of Aβ toxicity. H_2O_2 produced in tandem with the oxidation of cholesterol by Aβ:Cu^{2+} is likely to contribute to the toxicity we observed. While excess of either H_2O_2 (14) or 4-cholesten-3-one (the present study) alone is toxic to neurons in culture, recent reports indicate that H_2O_2 production by Aβ is necessary but not sufficient to mediate the toxicity of the peptide in culture (38, 41). Therefore, the simultaneous production of 2 toxic agents by Aβ (e.g., H_2O_2 and oxidized cholesterol) in the membrane vicinity may potentiate toxicity. By studying the toxicity of Aβ variants that produce H_2O_2 but are unable to attach to cell membrane (and therefore exhibit diminished 4-cholesten-3-one generation), we established that oxidation of a membrane component is needed for Aβ toxicity even when H_2O_2 is generated (Figure 4).

Our findings are in broad agreement with a recent report that detected 7-OH cholesterol as a catalytic reaction product of Aβ:Cu^{2+} and cholesterol (42). Whereas in our cell-free experiments we only detected 1 reaction product on TLC (Figure 1), our conditions were different from those in the previous report in that we did not use detergent and 150 mM NaCl (in contrast to no NaCl) was present in the reaction buffer. While we do not exclude the possibility that 7-OH cholesterol or other oxidized membrane components contribute to Aβ toxicity, the abnormal combination of Aβ with Cu^{2+} may be an upstream adverse event that leads to tandem oxidation reactions in vivo. Our findings, though, are the first to our knowledge to show that the degree of Aβ neurotoxicity in cell cultures (Figure 4) or accumulation in transgenic mouse or human brain (Figures 5 and 6) is significantly associated with the levels of 4-cholesten-3-one, a result concordant with a role for this neurotoxin as a pathogenic mediator.

The generation of H_2O_2 from cholesterol oxidation may also cause cortical lipid peroxidation, which generates various products that are increased in AD — such as hydroxynonenal (43) and F_2 isoprostanes (44) — and are linked to the accumulation of Aβ in both in vitro and in vivo models (45, 46).

To our knowledge, this is the first report of 4-cholesten-3-one detected in the brain, which may be a biomarker for Aβ toxic activity. Its presence in normal brain tissue at levels about 1.5% those of cholesterol (approximately 0.3 mg/g wet wt; Figure 5) suggests that its production alone may not be abnormal and may reflect a metabolic process similar to that of bile salt synthesis in the liver, where 4-cholesten-3-one is formed as an intermediate (47, 48). The markedly elevated levels of 4-cholesten-3-one in AD postmortem brain may originate from Aβ:Cu^{2+} activity, since a similar elevation was found in the brains of Aβ transgenic mice compared with littermate controls. The systemic production of an atherogenic form of oxidized cholesterol such as 4-cholesten-3-one may explain why transgenic mice overexpressing human Aβ have aortic arteriosclerosis that is not observed in the background strain (20).

Cholesterol oxidase is a bacterial flavoenzyme with no known mammalian counterpart (49), but an activity generating 4-cholesten-3-one in mammalian liver microsomes has been previously described (47). Our data show for the first time to our knowledge that there is also some 4-cholesten-3-one in normal human and mouse brain (Figure 5). Therefore, we cannot yet exclude the possibility that the increased 4-cholesten-3-one levels seen in AD and Aβ transgenic mouse brain (Figure 5) come from sources other than Aβ. Nevertheless, elevated levels of 4-cholesten-3-one in AD could contribute to both neuronal damage and arteriosclerosis. Synaptic plasma membranes are more vulnerable than non-neuronal membranes to 4-cholesten-3-one production, which inhibits synaptic CaMg ATPase activity and membrane interdigitation (50). Therefore, the elevated 4-cholesten-3-one levels in AD (Figure 5, A and B) may burden synaptic function and

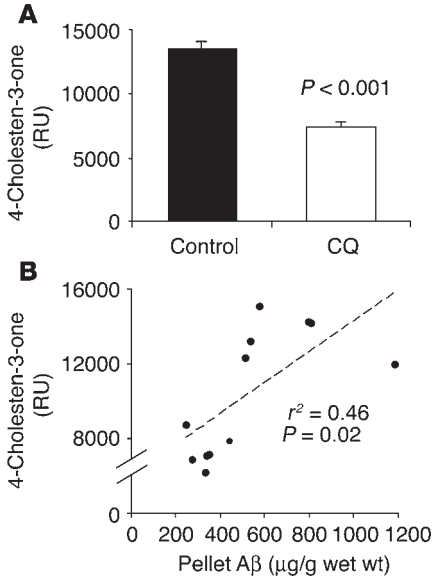

Figure 6
Treatment of APP transgenic mice with CQ decreased brain 4-cholesten-3-one levels. (**A**) Effect on 4-cholesten-3-one generation. Data are mean ± SEM of $n = 6$ transgenic mice per group. (**B**) Association of total Aβ levels extracted from the pellet phase of brain homogenates with 4-cholesten-3-one levels.

contribute to dementia. Brain 4-cholesten-3-one accumulation is implicated in the premature dementia of cerebrotendinous xanthomatosis (CTX), an autosomal-recessive condition caused by sterol 27–hydroxylase mutation (48). In CTX, liver 4-cholesten-3-one formed during bile salt synthesis transforms to cholestanol, which then deposits in the brain (47, 51, 52). Further studies will be needed to determine which cellular compartment contains the 4-cholesten-3-one and whether cholestanol also is increased in the brain in AD. Bacterial cholesterol oxidase–produced 4-cholesten-3-one is believed to exacerbate cardiovascular disease by increasing membrane fluidity (53). In the LDLs of patients with coronary artery disease, 4-cholesten-3-one levels are markedly elevated (2). The elevated 4-cholesten-3-one levels in Aβ transgenic mice may therefore explain the unusual presence of arteriosclerosis in these animals (20).

The cuproenzyme-like cholesterol oxidase activity of Aβ is a novel mechanism that unifies the toxicity of Aβ with cholesterol and copper abnormalities already associated with AD. $Aβ_{42}$ has more activity than $Aβ_{40}$ (Figure 1C), which correlates with its involvement in AD pathology and toxicity (14, 15). Other small peptides, including the mouse paralog of Aβ (which lacks a key redox-active tyrosine) (38), have been shown to be devoid of such catalytic redox activity (14, 15, 54). Unlike cholesterol oxidase activity, flavin adenine dinucleotide (FAD) is not required for the oxidation catalyzed by $Aβ:Cu^{2+}$. Inhibition of $Aβ:Cu^{2+}$ cholesterol oxidase activity (Figure 1C) may contribute to the mechanism by which CQ and related compounds inhibit brain Aβ accumulation in transgenic mice (27, 40), rescue Aβ-mediated neuronal toxicity (37), and prevent cognitive decline in AD patients (28).

Despite evidence for pro-oxidant $Aβ:Cu^{2+}$ accumulating in the brain in AD, the mechanism for its formation is uncertain but is not a simple product of age-dependent copper elevation in brain tissue (55–57). Increasing evidence indicates that Aβ and APP may constitutively handle copper and export it from the cell (55–59). Aβ is redox silent when bound to Cu^{2+} as a lipid-embedded complex, and oxidation of this complex may lead to abnormal lipid integration and the release of redox activity (12, 60).

At least 4 potential mechanisms that can link AD to cholesterol have already been identified: (a) clustering of APP and β-site amyloid precursor protein–cleaving enzyme 1 (BACE1) into lipid rafts, which facilitates β cleavage of APP (61); (b) intracellular cholesterol distribution, which is able to activate the amyloidogenic processing of APP (62, 63); (c) ozonolysis of cholesterol, which generates peroxi-derivatives of cholesterol that accelerate the aggregation of Aβ monomers (16), and (d) activity of α-secretase ADAM10 at the cell surface, which has been related to cholesterol levels (64). Here, we have added a new candidate to the above list, a novel enzymatic activity of the Aβ peptide that may be activated by age-dependent redistribution of brain copper (55).

In conclusion, elevated cholesterol levels may be a direct risk factor for AD — by providing substrate for Aβ-mediated oxidation — rather than being linked indirectly (e.g., through cardiovascular disease). Aβ cholesterol oxidase activity also may contribute to the recently described increased atheroma in APP transgenic mice (20). Inhibiting the production of cholesterol (e.g., with statins) may limit the oxidation of cholesterol by Aβ and so decrease risk for AD. However, new drugs inhibiting Aβ cholesterol oxidase activity, such as compounds similar to CQ, also hold potential.

Methods

In vitro oxidation. Free cholesterol (Sigma-Aldrich) was dissolved in chloroform, dried under nitrogen, redissolved in ethanol, and brought into PBS (24 volumes of PBS, pH 7.4, per volume of ethanol extract) by sonication. HPLC-grade water treated with Chelex (Bio-Rad Laboratories) was used in all experiments. For the initial in vitro experiments, cholesterol (50 μM) was incubated with freshly prepared Aβ (1 μM, W.M. Keck Laboratory, Yale University), Cu^{2+} (2 μM with 12 μM glycine), or both ($Aβ:Cu^{2+}$ complex) for 2 hours at 37°C. We used a $Cu^{2+}/Aβ$ ratio of 2:1 because Aβ has 2 Cu^{2+} binding sites that support redox activity (15). The reaction was stopped by adding chloroform and methanol (sample/chloroform/methanol, 1:4:2 vol/vol/vol) followed by Folsch extraction. For the kinetic curve, increasing concentrations of cholesterol were incubated with Aβ (200 nM) and Cu^{2+} (400 nM) with glycine (2,400 nM) for 60 minutes. A low concentration of EDTA (10 μM) was included to prohibit contaminating concentrations (less than 0.2 μM) of free Cu^{2+} or Fe^{3+} from contributing to the reactions. In some experiments, cholesterol was also incubated (50 μM, 25°C for 30 minutes) in the presence of 1 μM BSA complexed with 2 μM Cu^{2+} and 12 μM glycine as a negative control or 5 IU cholesterol oxidase purified from *Pseudomonas fluorescens* (Sigma-Aldrich) as a positive control. CQ was purchased from Spectrum Chemical Manufacturing Corp. and was made into a stock solution of 100 μM in ethanol. All reagents were checked for metal contamination, which is most commonly observed with EDTA stocks and DMSO.

Neuronal cell culture oxidation. Neuronal cultures, derived from hippocampi and frontal cortices from E16–E18 mice, were prepared as described previously (62). All animal experiments were approved by the Subcommittee on Research Animal Care, Massachusetts General Hospital. Neurons were first incubated with [^{14}C]–acetic acid (57.0 Ci/mol^{-1}; Amersham Biosciences) for 3 days ad equilibrium to allow steady-state labeling of cellular cholesterol, then washed twice with Neurobasal medium (Invitrogen Corp.) and incubated with Neurobasal lacking antioxidants but containing 2% B27 supplements. For treatment of neuronal cultures, fresh $Aβ_{42}$ (200 nM) was added together with Cu^{2+} (400 nM) plus glycine (2,400 nM) and EDTA (10 μM, to exclude oxidation mediated by free Cu^{2+}), and the mixture was incubated with the cells in

culture for up to 3 days. At the end of this period the cells were centrifuged in order to analyze adherent and nonadherent cells for cholesterol oxidation and apoptosis. Cell viability was analyzed using the LDH assay of culture medium (Sigma-Aldrich), while apoptotic activation was analyzed using monoclonal antibody C-2-10 against PARP (BD Biosciences — Clontech).

Analysis of cholesterol oxides. Samples were obtained by Folsch extraction in chloroform/methanol (sample/chloroform/methanol, 1:4:2 vol/vol/vol) by vortexing overnight at 4°C. The chloroform phase was separated by centrifugation (1,000 *g* for 15 minutes), dried, resuspended in chloroform (0.5 ml), and then applied to a Silica Gel-G TLC plate (EMD Chemicals). Plates were developed in a mobile phase of hexane/ethyl ether/acetic acid (87:20:1 vol/vol/vol) and compounds were stained with iodine vapor for analysis. R*f* values were compared to the R*f* of pure standards of cholesterol and 4-cholesten-3-one (Sigma-Aldrich). Pixel densities from developed TLC plates were calculated from scanned images with Adobe Photoshop version 7.0, and values were compared with those of standards. For quantification of the radioactive species of cholesterol, samples were applied to the TLC plates in parallel channels together with standards (Sigma-Aldrich). The migrating spots corresponding to free cholesterol and 4-cholesten-3-one were scraped and counted. Control studies with pure cholesterol and [^{3}H]cholesterol confirmed that Folsch extraction and TLC alone did not lead to the generation of 4-cholesten-3-one.

Analysis of cholesterol oxides from human brain. Inferior parietal cortex was examined from cases with AD (Braak stage VI/VI; autopsy-confirmed human tissue supplied by the Harvard Human Tissue Resource Center) and compared with tissue from the same brain region from control subjects (PD, AC, and YC). Tissue (750 mg) was homogenized in PBS (750 μl) containing protease inhibitors (Roche Diagnostics Corp.), then obtained for TLC by Folsch extraction.

Transgenic mice. Tg2576 mice were propagated via backcrossing to an F_1 cross between SJL and C57BL/6 mice; all mouse strains were obtained from Taconic as previously described (65). Seventeen-month-old animals (4 male and 4 female non-Tg, 4 male and 8 female Tg) were analyzed for 4-cholesten-3-one levels. For the effects of CQ treatment upon brain 4-cholesten-3-one levels, 21-month-old animals were treated for 9 weeks with CQ (3 male and 3 female) or vehicle alone (3 male and 3 female) by gavage, as previously described (27).

GC-MS identification of 4-cholesten-3-one in brain. Extracts of autopsy material were run on TLC plates containing standards in parallel lanes and visualized by iodine staining. The spot corresponding to the unknown sterol was cut from the plate, scraped into a glass vial, and sonicated in chloroform/methanol (2 ml, 1:1 vol/vol) to elute the compound for characterization by GC-MS. This sample was concentrated to 50 μl by evaporation under nitrogen. A portion (5 μl) of this sample was taken for direct analysis by GC-MS. The remaining sample was converted to the methyloxime derivative (32) after evaporation to dryness under nitrogen, addition of 100 μl of dry redistilled pyridine and 5 mg of methoxyamine hydrochloride, and heating at 60°C for 30 minutes. After derivatization, the sample was evaporated to dryness under a stream of nitrogen gas and then the derivative dissolved in hexane (50 μl) and analyzed by GC-MS (34).

GC-MS was performed on an Autospec Q high-resolution mass spectrometer (Waters Corp.) housing a 30-m by 0.32-mm DB-1 (0.25 μm film thickness) fused silica column using temperature-programmed operation from 185°C to 295°C at increments of 2°C per minute with initial and final isothermal periods of 2 minutes and 30 minutes, respectively. Electron ionization (70 electron volts) mass spectra were obtained by repetitive scanning of the mass range 50–1,000 amu throughout the elution of compounds from the GC column. The identification of 4-cholesten-3-one was established by comparing the retention index of the underivatized and methyloxime derivative of the compound, measured relative to a homologous series of n-alkanes (quoted as MU) and the electron ionization mass spectrum with the pure standard of 4-cholesten-3-one.

Statistical analysis. Unless otherwise indicated, values are given as mean ± SEM. ANOVA was used to compare groups, followed by post-hoc *t* test, with $P < 0.05$ considered statistically significant.

Acknowledgments

This work was supported by grants from the National Institute on Aging (AG12686 to A.I. Bush and AG18679 to S. Melov), the Alzheimer's Association (to L. Puglielli and A.I. Bush), the National Health and Medical Research Council (to A.I. Bush), the Institute for the Study of Aging (to S. Melov), and the National Institute of Neurological Disorders and Stroke (to D.M. Kovacs and postdoctoral fellowship grant F32NS10874 to A.L. Friedlich). Tissue was supplied by the Harvard Brain Tissue Resource Center (supported by grant R24MH68855 from the National Institute of Mental Health). We thank Tobias Hartmann for helpful suggestions.

Received for publication October 13, 2004, and accepted in revised form June 14, 2005.

Address correspondence to: Ashley I. Bush, Mental Health Research Institute of Victoria, 155 Oak Street, Parkville 3052, Victoria, Australia. Phone: 61-39389-2962; Fax: 61-39387-5061; E-mail: bush@helix.mgh.harvard.edu.

Luigi Puglielli's present address is: Department of Medicine, University of Wisconsin-Madison, and Veteran's Administration Hospital, Madison, Wisconsin, USA.

Seiichi Nagano's present address is: Department of Neurology, Osaka University Graduate School of Medicine, Suita, Japan.

Luigi Puglielli and Avi L. Friedlich contributed equally to this work.

1. Bhadra, S., et al. 1991. Oxidation of cholesterol moiety of low density lipoprotein in the presence of human endothelial cells or Cu+2 ions: identification of major products and their effects. *Biochem. Biophys. Res. Commun.* **176**:431–440.
2. Liu, K.Z., Cuddy, T.E., and Pierce, G.N. 1992. Oxidative status of lipoproteins in coronary disease patients. *Am. Heart J.* **123**:285–290.
3. Chang, Y.H., Abdalla, D.S., and Sevanian, A. 1997. Characterization of cholesterol oxidation products formed by oxidative modification of low density lipoprotein. *Free Radic. Biol. Med.* **23**:202–214.
4. Brown, A.J., et al. 2000. Cholesterol and oxysterol metabolism and subcellular distribution in macrophage foam cells. Accumulation of oxidized esters in lysosomes. *J. Lipid Res.* **41**:226–237.
5. Launer, L.J., White, L.R., Petrovitch, H., Ross, G.W., and Curb, J.D. 2001. Cholesterol and neuropathologic markers of AD: a population-based autopsy study. *Neurology.* **57**:1447–1452.
6. Pappolla, M.A., et al. 2002. Cholesterol, oxidative stress, and Alzheimer's disease: expanding the horizons of pathogenesis [review]. *Free. Radic. Biol. Med.* **33**:173–181.
7. Smith, C.D., et al. 1991. Excess brain protein oxidation and enzyme dysfunction in normal aging and Alzheimer's disease. *Proc. Natl. Acad. Sci. U. S. A.* **88**:10540–10543.
8. Nunomura, A., et al. 2001. Oxidative damage is the earliest event in Alzheimer disease. *J. Neuropathol. Exp. Neurol.* **60**:759–767.
9. Smith, M.A., et al. 1998. Amyloid-beta deposition in Alzheimer transgenic mice is associated with oxidative stress. *J. Neurochem.* **70**:2212–2215.
10. Atwood, C.S., et al. 1998. Dramatic aggregation of Alzheimer Aβ by Cu(II) is induced by conditions representing physiological acidosis. *J. Biol. Chem.* **273**:12817–12826.
11. Atwood, C.S., et al. 2000. Characterization of copper interactions with Alzheimer amyloid beta peptides: identification of an attomolar-affinity copper binding site on amyloid beta1-42. *J. Neurochem.* **75**:1219–1233.
12. Curtain, C., et al. 2001. Alzheimer's disease amyloid-beta binds copper and zinc to generate an allosterically ordered membrane-penetrating structure containing superoxide dismutase-like subunits. *J. Biol. Chem.* **276**:20466–20473.

13. Curtain, C.C., et al. 2003. Metal ions, pH, and cholesterol regulate the interactions of Alzheimer's disease amyloid-beta peptide with membrane lipid. *J. Biol. Chem.* **278**:2977–2982.
14. Huang, X., et al. 1999. Cu(II) potentiation of Alzheimer Abeta neurotoxicity. Correlation with cell-free hydrogen peroxide production and metal reduction. *J. Biol. Chem.* **274**:37111–37116.
15. Opazo, C., et al. 2002. Metalloenzyme-like activity of Alzheimer's disease beta-amyloid: Cu-dependent catalytic conversion of dopamine, cholesterol and biological reducing agents to neurotoxic H_2O_2. *J. Biol. Chem.* **277**:40302–40308.
16. Zhang, Q., et al. 2004. Metabolite-initiated protein misfolding may trigger Alzheimer's disease. *Proc. Natl. Acad. Sci. U. S. A.* **101**:4752–4757.
17. Dietschy, J.M., and Turley, S.D. 2001. Cholesterol metabolism in the brain. *Curr. Opin. Lipidol.* **12**:105–112.
18. Mori, T., et al. 2001. Cholesterol accumulates in senile plaques of Alzheimer disease patients and in transgenic APP(SW) mice. *J. Neuropathol. Exp. Neurol.* **60**:778–785.
19. Refolo, L.M., et al. 2000. Hypercholesterolemia accelerates the Alzheimer's amyloid pathology in a transgenic mouse model. *Neurobiol. Dis.* **7**:321–331.
20. Li, L., Cao, D., Garber, D.W., Kim, H., and Fukuchi, K. 2003. Association of aortic atherosclerosis with cerebral beta-amyloidosis and learning deficits in a mouse model of Alzheimer's disease. *Am. J. Pathol.* **163**:2155–2164.
21. Lovell, M.A., Robertson, J.D., Teesdale, W.J., Campbell, J.L., and Markesbery, W.R. 1998. Copper, iron and zinc in Alzheimer's disease senile plaques. *J. Neurol. Sci.* **158**:47–52.
22. Dong, J., et al. 2003. Metal binding and oxidation of amyloid-beta within isolated senile plaque cores: Raman microscopic evidence. *Biochemistry.* **42**:2768–2773.
23. Navas, J., Gonzalez-Zorn, B., Ladron, N., Garrido, P., and Vazquez-Boland, J.A. 2001. Identification and mutagenesis by allelic exchange of choE, encoding a cholesterol oxidase from the intracellular pathogen Rhodococcus equi. *J. Bacteriol.* **183**:4796–4805.
24. Lario, P.I., Sampson, N., and Vrielink, A. 2003. Sub-atomic resolution crystal structure of cholesterol oxidase: what atomic resolution crystallography reveals about enzyme mechanism and the role of the FAD cofactor in redox activity. *J. Mol. Biol.* **326**:1635–1650.
25. DeGrella, R.F., and Simoni, R.D. 1982. Intracellular transport of cholesterol to the plasma membrane. *J. Biol. Chem.* **257**:14256–14262.
26. Gutteridge, J.M., and Wilkins, S. 1983. Copper salt-dependent hydroxyl radical formation. Damage to proteins acting as antioxidants. *Biochim. Biophys. Acta.* **759**:38–41.
27. Cherny, R.A., et al. 2001. Treatment with a copper-zinc chelator markedly and rapidly inhibits β-amyloid accumulation in Alzheimer's disease transgenic mice. *Neuron.* **30**:665–676.
28. Ritchie, C.W., et al. 2003. Metal-protein attenuation with iodochlorhydroxyquin (clioquinol) targeting Aβ amyloid deposition and toxicity in Alzheimer's disease: a pilot phase 2 clinical trial. *Arch. Neurol.* **60**:1685–1691.
29. Shapiro, R., and Djerassi, C. 1964. Mass spectrometry in structural and stereochemical problems. L. Fragmentation and hydrogen migration reactions of a,b-unsaturated 3-keto steroids. *J. Am. Chem. Soc.* **86**:2825–2832.
30. Djerassi, C., Karliner, J., and Aplin, R. 1965. Mass spectrometry in structural and stereochemical problems. LXXVIII. Steroidal D4-3,6-diketones. *Steroids.* **6**:1–8.
31. Smith, A., and Brooks, C. 1975. Mass spectra of D4- and 5a-3-ketosteroids formed during the oxidation of some 3b-hydroxysteroids by cholesterol oxidase. *Biomed. Mass Spectrom.* **3**:81–87.
32. Thenot, J.-P., and Horning, E. 1972. MO-TMS derivatives of human urinary steroids for GC and GC-MS studies. *Anal. Lett.* **5**:21–33.
33. Axelson, M., and Sjovall, J. 1978. Separation and configuration of syn and anti isomers of testosterone oxime. *Anal. Lett.* **B11**:229–237.
34. Setchell, K.D., Alme, B., Axelson, M., and Sjovall, J. 1976. The multicomponent analysis of conjugates of neutral steroids in urine by lipophilic ion exchange chromatography and computerised gas chromatography-mass spectrometry. *J. Steroid Biochem.* **7**:615–629.
35. Liu, K.Z., Maddaford, T.G., Ramjiawan, B., Kutryk, M.J., and Pierce, G.N. 1991. Effects of cholesterol oxidase on cultured vascular smooth muscle cells. *Mol. Cell. Biochem.* **108**:39–48.
36. Kellner-Weibel, G., Geng, Y.J., and Rothblat, G.H. 1999. Cytotoxic cholesterol is generated by the hydrolysis of cytoplasmic cholesteryl ester and transported to the plasma membrane. *Atherosclerosis.* **146**:309–319.
37. Abramov, A.Y., Canevari, L., and Duchen, M.R. 2003. Changes in intracellular calcium and glutathione in astrocytes as the primary mechanism of amyloid neurotoxicity. *J. Neurosci.* **23**:5088–5095.
38. Barnham, K.J., et al. 2004. Tyrosine gated electron transfer is key to the toxic mechanism of Alzheimer's disease beta-amyloid. *FASEB J.* **18**:1427–1429.
39. Tickler, A.K., et al. 2005. Methylation of the imidazole side chains of the Alzheimer disease amyloid-beta peptide results in abolition of superoxide dismutase-like structures and inhibition of neurotoxicity. *J. Biol. Chem.* **280**:13355–13363.
40. Lee, J.Y., Friedman, J.E., Angel, I., Kozak, A., and Koh, J.Y. 2004. The lipophilic metal chelator DP-109 reduces amyloid pathology in brains of human beta-amyloid precursor protein transgenic mice. *Neurobiol. Aging.* **25**:1315–1321.
41. Ciccotosto, G.D., et al. 2004. Enhanced toxicity and cellular binding of a modified amyloid peptide with a methionine to valine substitution. *J. Biol. Chem.* **279**:42528–42534.
42. Nelson, T.J., and Alkon, D.L. 2005. Oxidation of cholesterol by amyloid precursor protein and beta-amyloid peptide. *J. Biol. Chem.* **280**:7377–7387.
43. Sayre, L.M., et al. 1997. 4-Hydroxynonenal-derived advanced lipid peroxidation end products are increased in Alzheimer's disease. *J. Neurochem.* **68**:2092–2097.
44. Pratico, D., et al. 2000. Increased 8,12-iso-iPF2alpha-VI in Alzheimer's disease: correlation of a non-invasive index of lipid peroxidation with disease severity. *Ann. Neurol.* **48**:809–812.
45. Mark, R.J., Lovell, M.A., Markesbery, W.R., Uchida, K., and Mattson, M.P. 1997. A role for 4-hydroxynonenal, an aldehydic product of lipid peroxidation, in disruption of ion homeostasis and neuronal death induced by amyloid β-peptide. *J. Neurochem.* **68**:255–264.
46. Pratico, D., Uryu, K., Leight, S., Trojanoswki, J.Q., and Lee, V.M. 2001. Increased lipid peroxidation precedes amyloid plaque formation in an animal model of Alzheimer amyloidosis. *J. Neurosci.* **21**:4183–4187.
47. Bjorkhem, I., and Karlmar, K.E. 1974. Biosynthesis of cholestanol: conversion of cholesterol into 4-cholesten-3-one by rat liver microsomes. *Biochim. Biophys. Acta.* **337**:129–131.
48. Cali, J.J., Hsieh, C.L., Francke, U., and Russell, D.W. 1991. Mutations in the bile acid biosynthetic enzyme sterol 27-hydroxylase underlie cerebrotendinous xanthomatosis. *J. Biol. Chem.* **266**:7779–7783.
49. MacLachlan, J., Wotherspoon, A., Ansell, R., and Brooks, C. 2000. Cholesterol oxidase: sources, physical properties and analytical applications [review]. *J. Steroid Biochem. Mol. Biol.* **72**:169–195.
50. Wood, W.G., Igbavboa, U., Rao, A.M., Schroeder, F., and Avdulov, N.A. 1995. Cholesterol oxidation reduces Ca(2+)+MG (2+)-ATPase activity, interdigitation, and increases fluidity of brain synaptic plasma membranes. *Brain Res.* **683**:36–42.
51. Menkes, J.H., Schimschock, J.R., and Swanson, P.D. 1968. Cerebrotendinous xanthomatosis. The storage of cholestanol within the nervous system. *Arch. Neurol.* **19**:47–53.
52. Salen, G., Shefer, S., and Tint, G.S. 1984. Transformation of 4-cholesten-3-one and 7 alpha-hydroxy-4-cholesten-3-one into cholestanol and bile acids in cerebrotendinous xanthomatosis. *Gastroenterology.* **87**:276–283.
53. Ghoshroy, K.B., Zhu, W., and Sampson, N.S. 1997. Investigation of membrane disruption in the reaction catalyzed by cholesterol oxidase. *Biochemistry.* **36**:6133–6140.
54. Huang, X., et al. 1999. The Aβ peptide of Alzheimer's disease directly produces hydrogen peroxide through metal ion reduction. *Biochemistry.* **38**:7609–7616.
55. Maynard, C.J., et al. 2002. Overexpression of Alzheimer's disease β-amyloid opposes the age-dependent elevations of brain copper and iron levels. *J. Biol. Chem.* **277**:44670–44676.
56. Bayer, T.A., et al. 2003. Dietary Cu stabilizes brain superoxide dismutase 1 activity and reduces amyloid Abeta production in APP23 transgenic mice. *Proc. Natl. Acad. Sci. U. S. A.* **100**:14187–14192.
57. Phinney, A.L., et al. 2003. In vivo reduction of amyloid-beta by a mutant copper transporter. *Proc. Natl. Acad. Sci. U. S. A.* **100**:14193–14198.
58. White, A.R., et al. 1999. Copper levels are increased in the cerebral cortex and liver of APP and APLP2 knockout mice. *Brain Res.* **842**:439–444.
59. Bellingham, S.A., et al. 2004. Gene knockout of amyloid precursor protein and amyloid precursor-like protein-2 increases cellular copper levels in primary mouse cortical neurons and embryonic fibroblasts. *J. Neurochem.* **91**:423–428.
60. Barnham, K.J., et al. 2003. Neurotoxic, redox-competent Alzheimer's beta-amyloid is released from lipid membrane by methionine oxidation. *J. Biol. Chem.* **278**:42959–42965.
61. Ehehalt, R., Keller, P., Haass, C., Thiele, C., and Simons, K. 2003. Amyloidogenic processing of the Alzheimer beta-amyloid precursor protein depends on lipid rafts. *J. Cell Biol.* **160**:113–123.
62. Puglielli, L., et al. 2001. Acyl-coenzyme A: cholesterol acyltransferase modulates the generation of the amyloid beta-peptide. *Nat. Cell Biol.* **3**:905–912.
63. Hutter-Paier, B., et al. 2004. The ACAT inhibitor CP-113,818 markedly reduces amyloid pathology in a mouse model of Alzheimer's disease. *Neuron.* **44**:227–238.
64. Kojro, E., Gimpl, G., Lammich, S., Marz, W., and Fahrenholz, F. 2001. Low cholesterol stimulates the nonamyloidogenic pathway by its effect on the alpha-secretase ADAM 10. *Proc. Natl. Acad. Sci. U. S. A.* **98**:5815–5820.
65. Callahan, M.J., et al. 2001. Augmented senile plaque load in aged female beta-amyloid precursor protein-transgenic mice. *Am. J. Pathol.* **158**:1173–1177.